

Fission characteristics of the excited compound nucleus ^{210}Rn in the framework of the four-dimensional dynamical model

H. Eslamizadeh* and E. Ahadi

Department of Physics, Faculty of Basic Sciences, Persian Gulf University, P.O. Box 7516913817, Bushehr, Iran

(Received 26 August 2017; published 27 September 2017)

The evaporation residue cross section, the anisotropy of the fission fragments angular distribution, the fission probability, the mass-energy distribution of the fission fragments, and the average pre-scission neutron multiplicity have been calculated for the compound nucleus ^{210}Rn by using four-dimensional Langevin equations with dissipation generated through the chaos-weighted wall and window friction formula. Three collective shape coordinates plus the projection of the total spin of the compound nucleus to the symmetry axis K were considered in the four-dimensional dynamical model. In the dynamical calculations dissipation coefficient of K , γ_k was considered as a free parameter, and its magnitude was inferred by fitting measured data on the evaporation residue cross section and the anisotropy of the fission fragments angular distribution for the compound nucleus ^{210}Rn . It was shown that the results of the calculations are in good agreement with the experimental data by using values of the dissipation coefficient of K , equal to $\gamma_k = (0.185 - 0.200) (\text{MeV zs})^{-1/2}$. It also was shown that the influence of the dissipation coefficient of K on the results of the calculations of the fission probability, the mass-energy distribution of the fission fragments, and the average pre-scission neutron multiplicity for the compound nucleus ^{210}Rn is small.

DOI: [10.1103/PhysRevC.96.034621](https://doi.org/10.1103/PhysRevC.96.034621)

I. INTRODUCTION

The discovery of nuclear fission opened an important chapter in the study of nuclear physics, and many studies about heavy-ion fusion-fission reactions were performed theoretically and experimentally over the years. During the past decades different statistical and dynamical models have been applied extensively to elucidate many problems of the fission process of the excited nuclei produced in fusion reactions. Many authors, for the description of different features of fusion-fission reactions in statistical or dynamical models, assumed that compound nuclei have zero spin about the symmetry axis where this assumption is not correct as first pointed out by Lestone in Ref. [1]. The authors in Ref. [2] also stressed that a large volume of heavy-ion-induced fission data needs to be reanalyzed with considering the effect of the orientation degree of freedom.

In dynamical models the Langevin equations have been used extensively to simulate the fission process of the excited nuclei [3–20]. One-dimensional Langevin calculations can yield particle multiplicity, fission probability, and the distributions of the fission events with respect to the fission lifetime [21,22]. Two-dimensional Langevin calculations make it possible to calculate energy distribution for symmetric fission [23–25], and other features of the fission of heavy excited compound nuclei can be calculated on the basis of the three-dimensional (3D) Langevin calculations. Recently, four-dimensional (4D) Langevin equations by considering the dissipation coefficients for the orientation degree of freedom, the K coordinate, have been used to calculate different aspects of fusion-fission reactions [26–28]. It should be mentioned that accounting dynamically for the fluctuation of the K degree of freedom was first considered in Ref. [2].

The main purpose of this paper is to study of the effect of the nuclear dissipation coefficient of K on different aspects of fission of the excited compound nucleus ^{210}Rn produced in the reaction $^{16}\text{O} + ^{194}\text{Pt}$. In the present paper we use a constant and a nonconstant dissipation coefficient of K in the four-dimensional dynamical model to calculate the evaporation residue cross section, the anisotropy of the fission fragments angular distribution, the fission probability, the mass-energy distribution of the fission fragments, and the average pre-scission neutron multiplicity for the compound nucleus ^{210}Rn . The present paper has been arranged as follows. In Sec. II, we describe the models and basic equations. The results of the calculations are presented in Sec. III. Finally, the concluding remarks are given in Sec. IV.

II. DETAILS OF THE MODEL AND BASIC EQUATIONS

Nuclear shapes can be described in terms of the well-known c, h, α parametrization [29]. This parametrization was used successfully both in static and in dynamical calculations. In cylindrical coordinates the surface of the nucleus can be given by

$$\rho_s^2 = \begin{cases} (c^2 - z^2)(A_s + Bz^2/c^2 + \alpha z/c), & B \geq 0, \\ (c^2 - z^2)(A_s + \alpha z/c) \exp(Bcz^2), & B < 0, \end{cases} \quad (1)$$

where z is the coordinate along the symmetry axis and ρ_s is the radial coordinate of the nuclear surface. In Eq. (1) the quantities B and A_s are defined by

$$B = 2h + \frac{c-1}{2}, \quad (2)$$

$$A_s = \begin{cases} c^{-3} - \frac{B}{5}, & B \geq 0, \\ -\frac{4}{3} \frac{B}{\exp(Bc^3) + \left(1 + \frac{1}{2Bc^3}\right) \sqrt{-\pi Bc^3} \text{erf} \sqrt{-Bc^3}}, & B < 0, \end{cases} \quad (3)$$

*Corresponding author: eslamizadeh@pgu.ac.ir

where $\text{erf}(x)$ is the error function. In the present investigation, we use the 4D dynamical model based on Langevin equations to simulate the fission process of the compound nucleus ^{210}Rn produced in the reaction $^{16}\text{O} + ^{194}\text{Pt}$. In our calculations, we use the variables $\mathbf{q} = (q_1, q_2, q_3)$ as collective coordinates, which are connected with the shape parameters c , h , and α as follows:

$$\begin{aligned} q_1 &= c, \\ q_2 &= \left(h + \frac{3}{2} \right) / \left(\frac{5}{2c^3} + \frac{1-c}{4} + \frac{3}{2} \right), \\ q_3 &= \alpha / (A_s + B), \quad \text{if } B \geq 0, \\ q_3 &= \alpha / A_s, \quad \text{if } B < 0. \end{aligned} \quad (4)$$

The advantage of using the collective coordinates $\mathbf{q} = (q_1, q_2, q_3)$ instead of the (c, h, α) parameters was discussed in Ref. [30]. In our dynamical calculations, we use the 3D Langevin dynamical model, developed in Refs. [31–33], by adding the orientation degree of freedom (K coordinate) to three collective coordinates that describe the shape evolution of the fissioning nucleus. K is the projection of the total spin I to the symmetry (elongation) axis of the nucleus. The evolution of an excited nucleus can be considered within the stochastic approach as the motion of a Brownian particle placed in a viscous heat bath [34,35]. In our calculations, we use the Langevin equations as

$$\begin{aligned} \dot{q}_i &= \mu_{ij} p_j, \\ \dot{p}_i &= -\frac{1}{2} p_j p_k \frac{\partial \mu_{jk}}{\partial q_i} - \frac{\partial F}{\partial q_i} - \gamma_{ij} \mu_{jk} p_k + \theta_{ij} \xi_j. \end{aligned} \quad (5)$$

Here and below, there are summations over the repeated indices. In Eq. (5) $m_{ij} (\|\mu_{ij}\| = \|m_{ij}\|^{-1})$ is the tensor of inertia, $\mathbf{q} = (q_1, q_2, q_3)$ are the collective coordinates, $\mathbf{p} = (p_1, p_2, p_3)$ are the momenta conjugate to them, $F(\mathbf{q}, K) = V(\mathbf{q}, K) - a(\mathbf{q})T^2$ is the Helmholtz free energy, $V(\mathbf{q})$ is the potential energy, γ_{ij} is the friction tensor, $\theta_{ij} \xi_j$ is a random force, and θ_{ij} is its amplitude. The Markovian random forces have uncorrelated Gaussian distributions with zero mean values and the second moments determined by

$$\begin{aligned} \langle \xi_i \rangle &= 0, \\ \langle \xi_i(t_1) \xi_j(t_2) \rangle &= 2\delta_{ij} \delta(t_1 - t_2). \end{aligned} \quad (6)$$

The random force amplitudes are related to the diffusion tensor D_{ij} as follows:

$$D_{ij} = \theta_{ik} \theta_{kj}, \quad (7)$$

and the diffusion tensor satisfies the Einstein relation,

$$D_{ij} = T \gamma_{ij}. \quad (8)$$

The heat bath temperature T can be determined within the Fermi-gas model as [36]

$$T = \sqrt{E_{\text{int}}/a(\mathbf{q})}. \quad (9)$$

Here $a(\mathbf{q})$ is the level-density parameter, and E_{int} is the intrinsic excitation energy of the nucleus. The deformation dependence of the level-density parameter can be determined as [36]

$$a(\mathbf{q}) = 0.073A + 0.095A^{2/3} B_s(\mathbf{q}), \quad (10)$$

where B_s is the dimensionless functional of the surface energy in the liquid-drop model and A is the mass number of the fissile nucleus. As the nucleus moved toward the scission surface, the conservation of energy is satisfied by

$$E^* = E_{\text{int}}(t) + E_{\text{coll}}(\mathbf{q}, \mathbf{p}) + V(\mathbf{q}, K) + E_{\text{evap}}(t), \quad (11)$$

where $E_{\text{coll}} = 0.5\mu_{ij}(\mathbf{q})p_i p_j$ is the kinetic energy of the collective motion of the nucleus, $V(\mathbf{q}, K)$ is the potential energy of the compound nucleus, $E_{\text{evap}}(t)$ is the energy carried away by evaporated particles by time t , and E^* is the total excitation energy of the nucleus. In the dynamical calculations, dissipation is generated through the chaos-weighted wall and window friction formula, which is described in our previous paper [37]. For small elongation, before neck formation, the chaos-weighted wall formula is used to calculate the friction tensor, and after neck formation, the chaos-weighted wall and window friction formula is used. The inertia tensor is calculated in the Werner-Wheeler approximation for the incompressible and irrotational flow [38] as

$$m_{ij} = \pi \rho_m \int_{z_{\text{min}}}^{z_{\text{max}}} \rho_s^2(z) \left(A_i A_j + \frac{1}{8} \rho_s^2(z) A'_i A'_j \right) dz, \quad (12)$$

where the primes denote the differentiation with respect to z , ρ_m is the mass density of the nucleus, and z_{min} and z_{max} are the left and right ends of the nuclear shape. The expansion coefficients A_j are determined from the condition incompressibility of a compound nucleus where the time derivative of its volume must vanish. $A_j(z, q)$ can be given as

$$A_j(z, q) = -\frac{1}{\rho_s^2(z)} \frac{\partial}{\partial q_j} \int_{z_{\text{min}}}^z \rho_s^2(z') dz'. \quad (13)$$

The potential energy is calculated on the basis of the liquid-drop model with a finite range of nuclear forces [39] using the parameters from Ref. [40],

$$\begin{aligned} V(\mathbf{q}, I, K) &= [B_s(\mathbf{q}) - 1] E_s^0(A, Z) \\ &\quad + [B_c(\mathbf{q}) - 1] E_c^0(A, Z) + E_{\text{rot}}(\mathbf{q}, I, K), \end{aligned} \quad (14)$$

where E_s^0 and E_c^0 are the surface and Coulomb energies of a spherical nucleus, respectively. $B_s(\mathbf{q})$ and $B_c(\mathbf{q})$ are the surface and Coulomb energy terms, respectively. $B_s(\mathbf{q})$ and $B_c(\mathbf{q})$ can be calculated as in Ref. [39]. E_{rot} is the rotational energy of the nucleus. The rotational energy can be calculated by

$$E_{\text{rot}}(\mathbf{q}, I, K) = \frac{\hbar^2 I(I+1) - K^2}{2J_{\perp}(\mathbf{q})} + \frac{\hbar^2 K^2}{2J_{\parallel}(\mathbf{q})}. \quad (15)$$

The rigid body moments of inertia about and perpendicular to the symmetry axis can be calculated as follows [40]:

$$J_{\perp(\parallel)}(\mathbf{q}) = J_{\perp(\parallel)}^{\text{(sharp)}}(\mathbf{q}) + 4M_0 a_M^2, \quad (16)$$

where M_0 is the compound nucleus mass, $a_M = 0.704$ fm is the diffuseness parameter of the nuclear surface, and $J_{\perp(\parallel)}^{\text{(sharp)}}$ are the moments of inertia for a sharp-edged nuclear

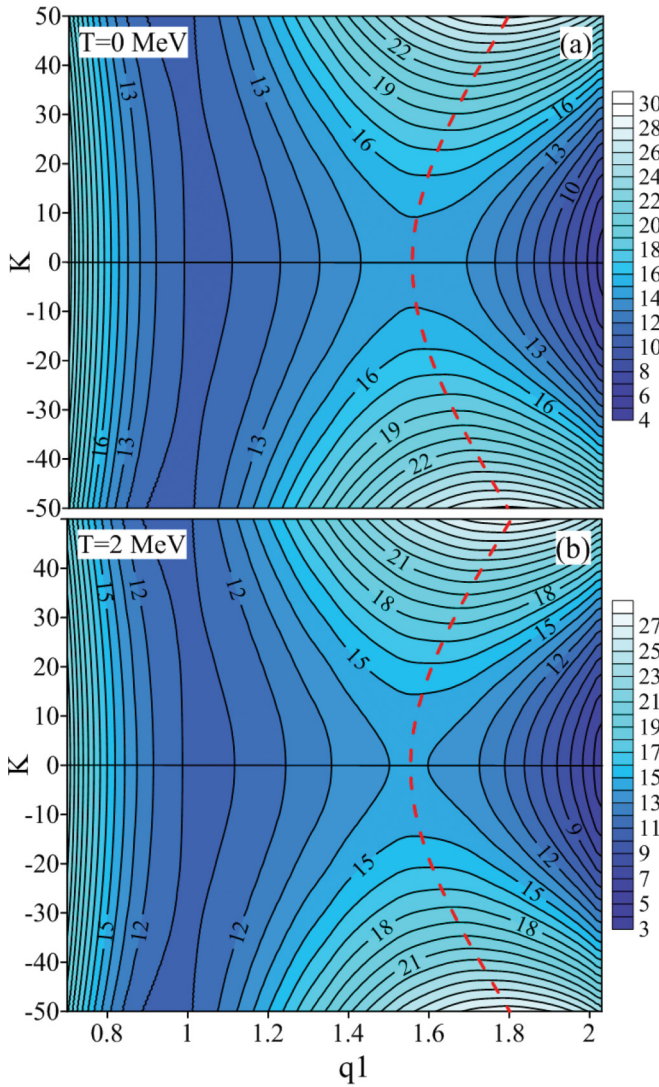


FIG. 1. The Helmholtz free energy for the compound nucleus ^{210}Rn as a function of the collective coordinates q_1 and K at $T = 0.0$, $T = 2.0$ MeV, and $I = 50\hbar$. The numbers on the contour lines represent the free energy values in MeV. The dashed curve shows the dependence of saddle-point deformations on K .

density distribution. The moments of inertia for a sharp-edged nuclear density distribution can be calculated as in Ref. [41]. Figures 1(a) and 1(b) show the Helmholtz free energy calculated for the compound nucleus ^{210}Rn as the function of the collective coordinate q_1 and for $T = 0.0$ and $T = 2.0$ MeV. It can be seen from Figs. 1(a) and 1(b) that the inclusion of the K coordinate changes not only the fission barrier height, but also it affects the saddle-point configuration. It also is clear from Figs. 1(a) and 1(b) that for a given value of spin the height of the fission barrier increases with increasing the value of K . Such an increase in the fission barrier will increase the fission time and consequently increase the number of evaporated prescission particles. Furthermore, it is clear from Figs. 1(a) and 1(b) that the height of the fission barrier decreases with increasing temperature of the nucleus.

It should be mentioned that many authors in their calculations for the description of different features of fusion-fission reactions assumed that the compound nuclei have zero spin about the symmetry axis. But, this assumption is not consistent with the statistical model and with the dynamical treatment of the orientation degree of freedom. The authors in Ref. [2] showed that the evolution of the K collective coordinate can be given as

$$dK = -\frac{\gamma_K^2 I^2}{2} \frac{\partial V}{\partial K} dt + \gamma_K I \xi(t) \sqrt{T} dt, \quad (17)$$

where γ_K is a parameter controlling the coupling between the orientation degree of freedom K and the heat bath, I is the spin of a compound nucleus, K is the projection of I on the symmetry axis of the nucleus, and $\xi(t)$ has the same meaning as in Eq. (5). The authors in Refs. [2,42] have shown that, in the case of a dinucleus, γ_K can be given as

$$\gamma_K = \frac{1}{RR_N \sqrt{2\pi^3 n_0}} \sqrt{\frac{J_R |J_{\text{eff}}| J_{\parallel}}{J_{\perp}^3}}, \quad (18)$$

where $J_R = M_0 R^2/4$ for a reflection symmetric shape and $n_0 = 0.0263 \text{ MeV zs fm}^{-4}$ is the bulk flux in the standard nuclear matter [43]. R_N is the neck radius, R is the distance between the centers of mass of the nascent fragments. J_{\parallel} and J_{\perp} are the rigid body moments of inertia about and perpendicular to the symmetry axis. J_{eff} is the effective moment of inertia. The effective moment of inertia can be calculated as

$$J_{\text{eff}} = \frac{J_{\parallel} J_{\perp}}{J_{\perp} - J_{\parallel}}. \quad (19)$$

By averaging Eq. (17), it can be shown that

$$\frac{d\langle K \rangle}{dt} = -\frac{\gamma_K^2 I^2}{2} \left\langle \frac{\partial V}{\partial K} \right\rangle. \quad (20)$$

From the expression for the rotational energy, it follows that:

$$\frac{d\langle K \rangle}{dt} = -\frac{\gamma_K^2 I^2 \hbar^2}{2J_{\text{eff}}} \langle K \rangle. \quad (21)$$

By assuming a constant γ_K , the solution of this equation has the form

$$\langle K(t) \rangle_{K_0} = K_0 \exp \left[-\frac{\gamma_K^2 I^2 \hbar^2}{2J_{\text{eff}}} (t - t_0) \right], \quad (22)$$

which gives the following expression for the relaxation time as

$$\tau_K = \frac{2J_{\text{eff}}}{\gamma_K^2 I^2 \hbar^2}. \quad (23)$$

In the simulation of the fission process of an excited compound nucleus the Langevin trajectories are simulated starting from the ground-state deformation with the excitation energy E^* of the compound nucleus. The initial conditions can be chosen by the Neumann method with the generating

function,

$$\Phi(\mathbf{q}_0, \mathbf{p}_0, I, t = 0) \propto \exp \left[-\frac{V(\mathbf{q}_0) + E_{\text{coll}}(\mathbf{q}_0, \mathbf{p}_0)}{T} \right] \times \delta(\mathbf{q} - \mathbf{q}_0) \delta(I - I_0). \quad (24)$$

In our calculations, we start modeling fission dynamics from the ground state with the excitation energy E^* of the compound nucleus. Evaporation of pre-scission light particles along the Langevin trajectory is taken into account using a Monte Carlo simulation technique. The decay widths for emission n, p, α, γ are calculated at each Langevin time step Δt as in Refs. [44,45]. The probabilities of decay via different channels can be calculated by using a standard Monte Carlo cascade procedure. In the simulation of the evolution of a fissile nucleus, a Langevin trajectory either reaches the scission surface and counts as a fission event or the intrinsic excitation energy becomes lower than the binding energy of a neutron or the height of the fission barrier counts as an evaporation residue event.

The spin distribution of the compound nucleus can be described by the formula,

$$\frac{d\sigma_{\text{Fus}}(I)}{dI} = \frac{2\pi}{k^2} \frac{2I + 1}{1 + \exp\left(\frac{I - I_c}{\delta I}\right)}, \quad (25)$$

where I_c is the critical spin and δI is the diffuseness. The parameters I_c and δI can be approximated as in Ref. [46].

In our calculations, it is assumed that the total kinetic energy E_k of the fission fragments is the sum of the nuclear attractive energy V_n of the nascent fragments, the Coulomb repulsion energy V_c of the fragments, and the kinetic energy of their relative motion E_{ps} . Therefore, the mean value of the total kinetic energy of the fission fragments can be defined as follows:

$$\langle E_k \rangle = \langle V_c \rangle + \langle V_n \rangle + \langle E_{ps} \rangle. \quad (26)$$

The fission fragment angular distributions can also be obtained by the following relation [47,48]:

$$W(\theta, I, K) = (I + 1/2) |D_{M=0, K}^I(\theta)|^2, \quad (27)$$

where θ is the angle with respect to the space fixed axis and $D_{M, K}^I(\theta)$ is the symmetric-top-wave function [47]. In the dynamical calculations, the fission fragment angular distributions can be obtained by averaging the expression Eq. (27) over the ensemble of the Langevin trajectories as follows:

$$W(\theta) = \frac{1}{N_f} \sum_{i=1}^{N_f} (I^i + 1/2) |D_{0, K^i}^{I^i}(\theta)|^2, \quad (28)$$

where upper index i determines the value of the corresponding quantity at the scission point for the i Langevin trajectory and N_f is the number of trajectories reaching the scission surface. The anisotropy of the fission fragment angular distributions can be defined as

$$A = \frac{\langle W(180^\circ) \rangle}{\langle W(90^\circ) \rangle}. \quad (29)$$

In the Langevin calculations, the fission rate is obtained by the formula,

$$r(t) = \frac{1}{N - N_f(t)} \frac{\Delta N_f(t)}{\Delta t}, \quad (30)$$

here $N_f(t)$ is the number of trajectories that underwent separation before the instant t , N is the total number of trajectories, and $\Delta N_f(t)$ is the number of trajectories that underwent separation within the time-interval $t \rightarrow t + \Delta t$.

III. RESULTS AND DISCUSSIONS

In the present investigation, we used a stochastic approach based on 4D Langevin equations to calculate the evaporation residue cross section, the anisotropy of the fission fragments angular distribution, the fission probability, the mass-energy distribution of the fission fragments, and the average pre-scission neutron multiplicity for the compound nucleus ^{210}Rn produced in the reaction $^{16}\text{O} + ^{194}\text{Pt}$. In the Langevin equations, dissipation is generated through the chaos-weighted wall and window friction formula. Furthermore, we used a constant dissipation coefficient of K , γ_k , and a nonconstant dissipation coefficient according to Eq. (18) to simulate the dynamics of nucleus fission of the compound nucleus ^{210}Rn . In the dynamical calculations with a constant dissipation coefficient of K , the magnitude of this parameter has been considered as a free parameter, and its magnitude inferred by fitting measured data on the evaporation residue cross section and anisotropy of the fission fragments angular distribution for the compound nucleus ^{210}Rn . Figures 2 and 3 show the results of the evaporation residue cross section and the anisotropy of the fission fragments angular distribution as a function of excitation energy for the compound nucleus ^{210}Rn calculated with the 4D-dynamical model and by using values of the dissipation coefficient of K equal to $\gamma_k = (0.185-0.200)(\text{MeV zs})^{-1/2}$ and with a nonconstant dissipation coefficient. It is clear from Figs. 2 and 3 that the results of the 4D-dynamical model by

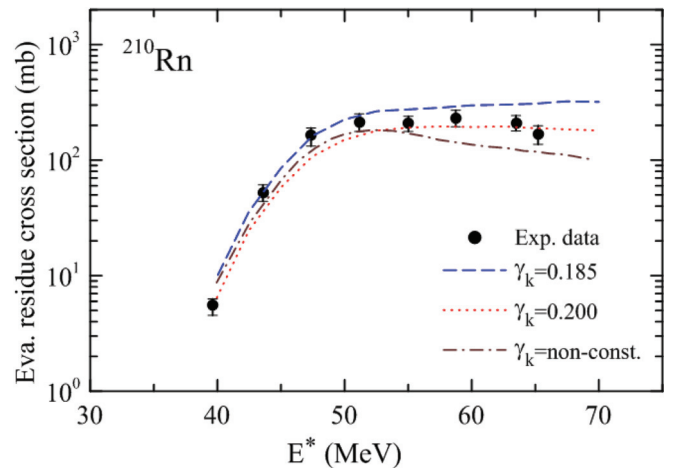


FIG. 2. The results of the evaporation residue cross section as a function of excitation energy for ^{210}Rn calculated with the 4D-dynamical model and by using different values of γ_k . The experimental data (filled circles) are taken from Ref. [49].

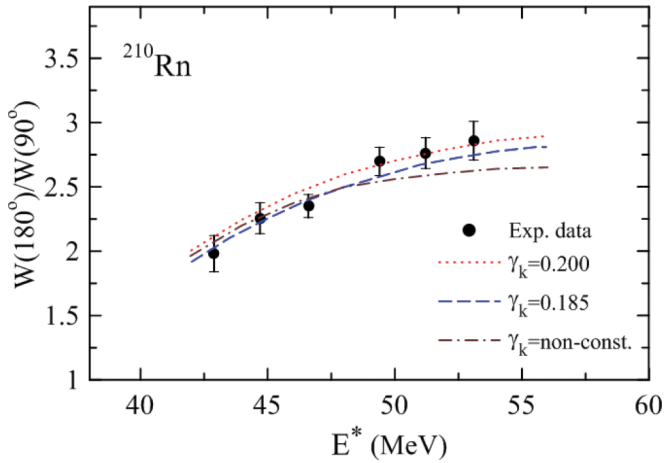


FIG. 3. The same as in Fig. 2 but for anisotropy of the fission fragment angular distribution as a function of excitation energy for ^{210}Rn . The filled circles are the experimental data [50].

using $\gamma_k = (0.185-0.200)(\text{MeV zs})^{-1/2}$ are in good agreement with the experimental data. It can also be seen from Figs. 2 and 3 that the dissipation coefficient for the orientation degree of freedom has an important influence on the results of the calculations. Furthermore, it is clear from Figs. 2 and 3 that the results of 4D Langevin equations together with a

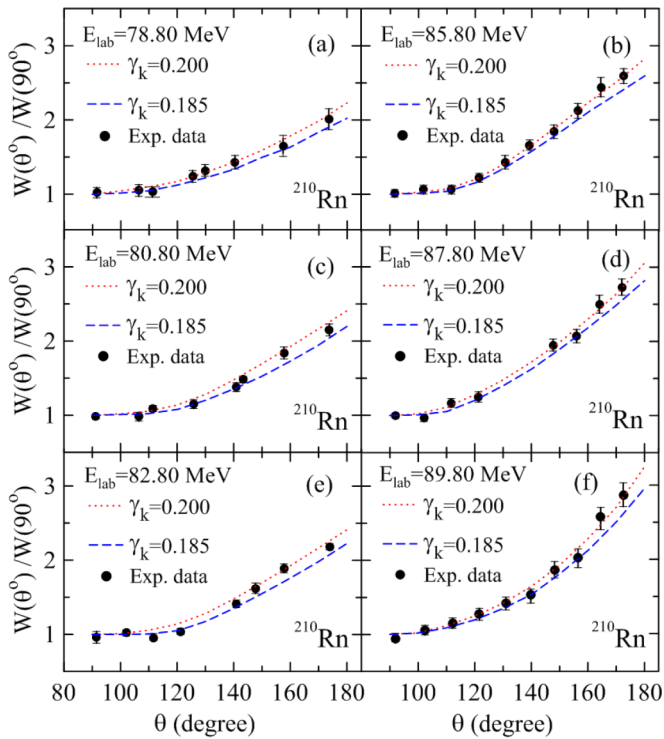


FIG. 4. The anisotropy of the fission fragment angular distributions for the compound nucleus ^{210}Rn as a function of scattering angle at different values of bombarding energies. The filled circles are the experimental data [50]. The dashed and dotted curves correspond to fitted values calculated with the 4D-dynamical model and by using different values of γ_k .

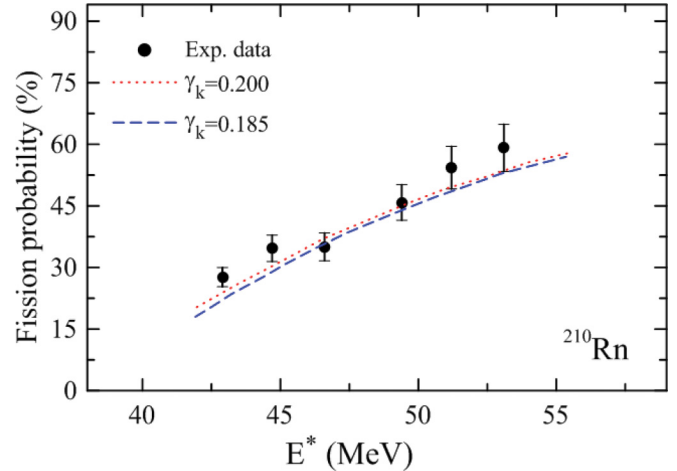


FIG. 5. The same as in Fig. 4 but for the fission probability as a function of excitation energy for ^{210}Rn . The filled circles are the experimental data [50].

nonconstant dissipation coefficient of K cannot accurately reproduce experimental data at higher excitation energies.

We also reproduced experimental data on the fission probability, average precession neutron multiplicity, and the anisotropy of fission fragment angular distribution as a function of scattering angle at bombarding energies $E_{\text{cm}} = 78.80, 80.80, 82.80, 85.80, 87.80,$ and 89.80 MeV to check the extracted values of the dissipation coefficient of K for the compound nucleus ^{210}Rn . Figures 4–6 show the results of the anisotropy of the fission fragment angular distribution, the fission probability, and the average precession neutron multiplicity for the compound nucleus ^{210}Rn . It can be seen from Figs. 4–6 that the results of the calculations calculated with the 4D-dynamical model and by using the values of the dissipation coefficient of K equal to $\gamma_k = (0.185-0.200)(\text{MeV zs})^{-1/2}$ can reproduce the experimental data. It also is clear from Figs. 5

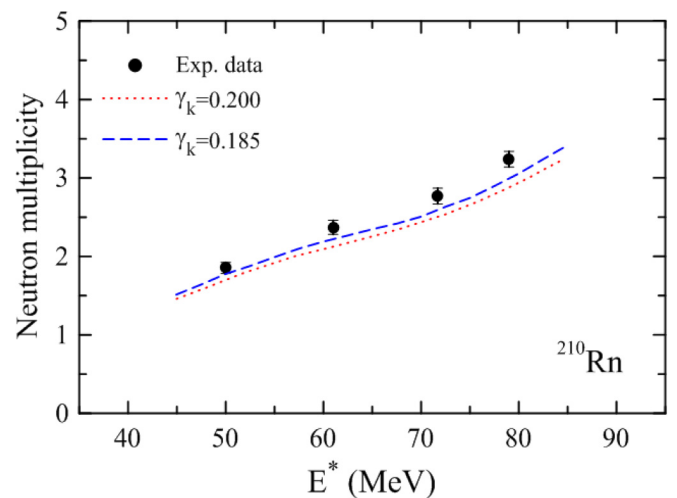


FIG. 6. The same as in Fig. 4 but for the average precession neutron multiplicity as a function of excitation energy for ^{210}Rn . The filled circles are the experimental data [51].

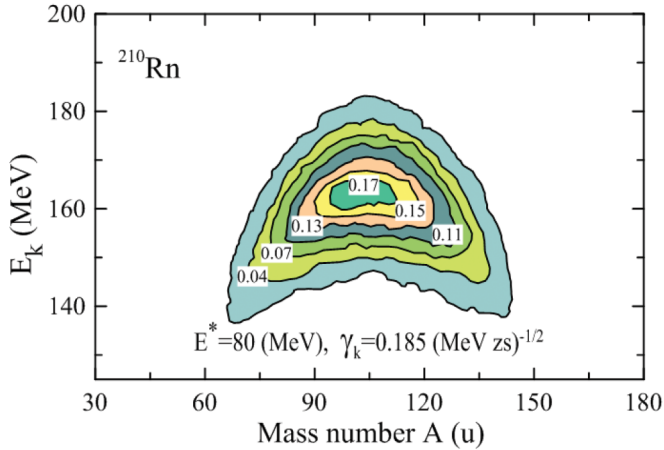


FIG. 7. A contour diagram of the mass-energy distribution of the fission fragments for the compound nucleus ^{210}Rn calculated with the 4D Langevin equations and by using $\gamma_k = 0.185(\text{MeV zs})^{-1/2}$ at $E^* = 80 \text{ MeV}$. The numbers on the contour lines are the yield of the fission fragments in percentages. The total yield is normalized for 200%.

and 6 that the influence of the dissipation coefficient of K on the results of the calculations of the fission probability and the average pre-scission neutron multiplicity for ^{210}Rn is small.

In the present investigation, we also calculated the mass-energy distribution of fission fragments $Y(E_K, M)$, based on 4D Langevin equations and by considering different values of the dissipation coefficient equal to $\gamma_k = (0.185-0.200)(\text{MeV zs})^{-1/2}$. Although, the difference between the results of the calculations of the mass-energy distribution of the fission fragments calculated by using different values of the dissipation coefficients of γ_k for ^{210}Rn is small. Figure 7 shows the contour plot of isolines for the mass-energy distribution of the fission fragments for the compound nucleus ^{210}Rn calculated by using $\gamma_k = 0.185(\text{MeV zs})^{-1/2}$ at $E^* = 80 \text{ MeV}$.

It can be seen from Fig. 7 that the shapes of the contour plots are close to being ellipsoidal in the region of the large values of $Y(E_K, M)$ and are similar to triangles in the region of small values of $Y(E_K, M)$.

Finally, we investigated the influence of the K coordinate on the fission rate of the compound nucleus ^{210}Rn at fixed spin $I = 30\hbar$ and at $E^* = 80 \text{ MeV}$. Figure 8 shows the fission rate of the compound nucleus ^{210}Rn as a function of time and by using different values of γ_k . It is clear from Fig. 8 that the fission rate increases with increasing the value of the dissipation coefficient of K . Such an increase in the fission rate decreases the fission time and increases the fission probability and consequently decreases the number of evaporated pre-scission particles.

It should be mentioned that, in our calculations in order to distinguish only the effect of the K coordinate on the fission rate, we performed the calculations with fixed spin

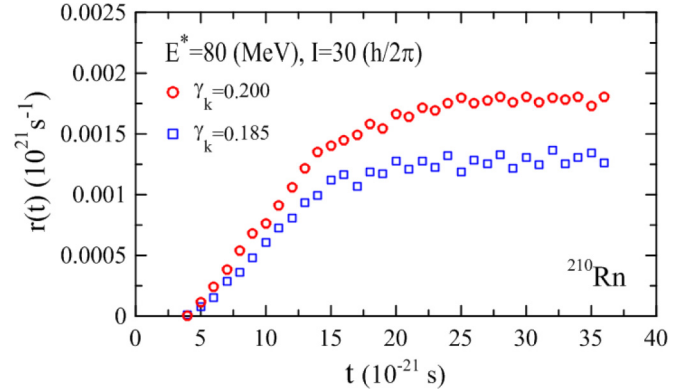


FIG. 8. The fission rate calculated for ^{210}Rn at fixed spin $I = 30\hbar$ and at $E^* = 80 \text{ MeV}$. The open squares and open circles are the calculated results calculated with the 4D Langevin equations and by using different values of the dissipation coefficient of K .

$I = 30\hbar$ and without taking into account the evaporation of the pre-scission particles.

IV. CONCLUSIONS

The evaporation residue cross section, the anisotropy of the fission fragments angular distribution, the fission probability, the average pre-scission neutron multiplicity, the mass-energy distribution of the fission fragments, and the fission rate have been calculated for the compound nucleus ^{210}Rn in the framework of the 4D-dynamical model and the results of the calculations compared with the experimental data. In our calculations, we used the chaos-weighted wall and window friction formula in the Langevin equations. Furthermore, in our calculations we used a constant dissipation coefficient of K and a nonconstant dissipation coefficient of K to reproduce the above-mentioned experimental data. Comparison of the calculated results with the experimental data showed that the results of the calculations are in good agreement with the experimental data by using values of the dissipation coefficient of K equal to $\gamma_k = (0.185-0.200)(\text{MeV zs})^{-1/2}$. It also was shown that the dissipation coefficient for the orientation degree of freedom has an important influence on the results of calculations. Although, the influence of the dissipation coefficient of K on the results of the calculations of the fission probability, the average pre-scission neutron multiplicity, and the mass-energy distribution of the fission fragments for ^{210}Rn is small.

ACKNOWLEDGMENT

Support of the Research Committee of the Persian Gulf University is greatly acknowledged.

[1] J. P. Lestone, *Phys. Rev. C* **59**, 1540 (1999).

[2] J. P. Lestone and S. G. McCalla, *Phys. Rev. C* **79**, 044611 (2009).

[3] P. N. Nadtochy, E. G. Ryabov, A. V. Cheredov, and G. D. Adeev, *Eur. Phys. J. A* **52**, 308 (2016).

- [4] E. G. Ryabov, A. V. Karpov, P. N. Nadtochy, and G. D. Adeev, *Phys. Rev. C* **78**, 044614 (2008).
- [5] V. Y. Denisov, T. O. Margitych, and I. Y. Sedykh, *Nucl. Phys. A* **958**, 101 (2017).
- [6] H. Eslamizadeh, *J. Phys. G: Nucl. Part. Phys.* **44**, 025102 (2017).
- [7] H. Eslamizadeh, *Eur. Phys. J. A* **50**, 186 (2014).
- [8] K. Mazurek, P. N. Nadtochy, E. G. Ryabov, and G. D. Adeev, *Eur. Phys. J. A* **53**, 79 (2017).
- [9] M. V. Chushnyakova and I. I. Gontchar, *Bull. Russ. Acad. Sci. Phys.* **80**, 938 (2016).
- [10] J. Tian, N. Wang, and W. Ye, *Phys. Rev. C* **95**, 041601 (2017).
- [11] H. Eslamizadeh, *Int. J. Mod. Phys. E* **24**, 1550052 (2015).
- [12] P. N. Nadtochy, A. Kelić, and K.-H. Schmidt, *Phys. Rev. C* **75**, 064614 (2007).
- [13] N. Vonta, G. A. Souliotis, M. Veselsky, and A. Bonasera, *Phys. Rev. C* **92**, 024616 (2015).
- [14] H. Eslamizadeh and H. Raanaei, *Ann. Nucl. Energy* **51**, 252 (2013).
- [15] H. Eslamizadeh, *J. Phys. G: Nucl. Part. Phys.* **40**, 095102 (2013).
- [16] W. Ye and J. Tian, *Phys. Rev. C* **93**, 044603 (2016).
- [17] W. Ye and J. Tian, *Phys. Rev. C* **91**, 064603 (2015).
- [18] H. Eslamizadeh, *Phys. Rev. C* **94**, 044610 (2016).
- [19] H. Eslamizadeh, *Int. J. Mod. Phys. E* **21**, 1250008 (2012).
- [20] H. Eslamizadeh and M. Soltani, *Ann. Nucl. Energy* **80**, 261 (2015).
- [21] Yu. A. Lazarev, I. I. Gontchar, and N. D. Mavlitov, *Phys. Rev. Lett.* **70**, 1220 (1993).
- [22] I. I. Gontchar, N. A. Ponomarenko, V. V. Turkin, and L. A. Litnevsky, *Phys. At. Nucl.* **67**, 2080 (2004).
- [23] G. I. Kosenko, D. V. Vanin, and G. D. Adeev, *Phys. At. Nucl.* **61**, 2031 (1998).
- [24] T. Wada, N. Carjan, and Y. Abe, *Nucl. Phys. A* **538**, 283 (1992).
- [25] G. R. Tillack, R. Reif, A. Schülke, P. Fröbrich, H. J. Krappe, and H. G. Reusch, *Phys. Lett. B* **296**, 296 (1992).
- [26] Y. A. Anisichenko, A. E. Gegechkori, and G. D. Adeev, *Acta Phys., Pol. B* **42**, 493 (2011).
- [27] P. N. Nadtochy, E. G. Ryabov, A. E. Gegechkori, Y. A. Anisichenko, and G. D. Adeev, *Phys. Rev. C* **89**, 014616 (2014).
- [28] P. N. Nadtochy, E. G. Ryabov, A. E. Gegechkori, Y. A. Anisichenko, and G. D. Adeev, *Phys. Rev. C* **85**, 064619 (2012).
- [29] M. Brack, J. Damgaard, A. S. Jensen, H. C. Puli, and V. M. Strutinsky, *Rev. Mod. Phys.* **44**, 320 (1972).
- [30] P. N. Nadtochy and G. D. Adeev, *Phys. Rev. C* **72**, 054608 (2005).
- [31] A. V. Karpov, R. M. Hiryanov, A. V. Sagdeev, and G. D. Adeev, *J. Phys. G: Nucl. Part. Phys.* **34**, 255 (2007).
- [32] P. N. Nadtochy, G. D. Adeev, and A. V. Karpov, *Phys. Rev. C* **65**, 064615 (2002).
- [33] A. V. Karpov, P. N. Nadtochy, D. V. Vanin, and G. D. Adeev, *Phys. Rev. C* **63**, 054610 (2001).
- [34] H. A. Kramers, *Physica* **7**, 284 (1940).
- [35] Y. Abe, C. Gregoire, and H. Delagrangé, *J. Phys. C: Solid State Phys.* **4**, 329 (1986).
- [36] A. V. Ignatyuk, M. G. Itkis, V. N. Okolovich, G. N. Smirenkin, and A. S. Tishin, *Yad. Fiz.* **21**, 1185 (1975).
- [37] H. Eslamizadeh, *J. Phys. G: Nucl. Part. Phys.* **39**, 085110 (2012).
- [38] K. T. R. Davies, A. J. Sierk, and J. R. Nix, *Phys. Rev. C* **13**, 2385 (1976).
- [39] H. J. Krappe, J. R. Nix, and A. J. Sierk, *Phys. Rev. C* **20**, 992 (1979).
- [40] A. J. Sierk, *Phys. Rev. C* **33**, 2039 (1986).
- [41] R. W. Hasse and W. D. Myers, *Geometrical Relationships of Macroscopic Nuclear Physics* (Springer-Verlag, Berlin/Heidelberg, 1988), p. 116.
- [42] S. G. McCalla and J. P. Lestone, *Phys. Rev. Lett.* **101**, 032702 (2008).
- [43] T. Døssing and J. Randrup, *Nucl. Phys. A* **433**, 215 (1985).
- [44] M. Blann, *Phys. Rev. C* **21**, 1770 (1980).
- [45] J. E. Lynn, *The Theory of Neutron Resonance Reactions* (Clarendon, Oxford, 1968), p. 325.
- [46] P. Fröbrich and I. I. Gontchar, *Phys. Rep.* **292**, 131 (1998).
- [47] R. Vandenbosch and J. R. Huizenga, *Nuclear Fission* (Academic, New York, 1973), p. 427.
- [48] A. Bohr and B. R. Mottelson, *Nuclear Structure* (World Scientific, Singapore, 1998), Vol. 2, p. 748.
- [49] E. Prasad *et al.*, *EPJ Web Conf.* **17**, 16011 (2011).
- [50] E. Prasad *et al.*, *Nucl. Phys. A* **882**, 62 (2012).
- [51] P. Sugathan *et al.*, *Phys. Rev. C* **87**, 014604 (2013).